

3D Soft Tissue Imaging: An Accurate and Economical Approach

Research Article

Dehis HM^{1*}, El-Sharaby FA², Mostafa YA³

¹ Assistant Lecturer, Faculty of Oral and Dental Medicine, Department of Orthodontics and Dentofacial Orthopedics, Cairo University, Egypt.

² Lecturer, Faculty of Oral and Dental Medicine, Department of Orthodontics and Dentofacial Orthopedics, Cairo University, Egypt.

³ Professor, Faculty of Oral and Dental Medicine, Department of Orthodontics and Dentofacial Orthopedics, Cairo University, Egypt.

Abstract

Research work regarding 3 dimensional (3D) soft tissue imaging is very scarce, the reason behind that is that 3D imaging modalities are either invasive, or expensive, or lack accuracy to a great extent.

Aim of the study: To develop a new, accurate and economical method for 3D soft tissue image construction to aid in the assessment of facial esthetics.

Materials and Methods: Ten adult females were comprised in the current study. For each subject, a 3D video model was constructed based on facial measurements taken after patient positioning using custom made patient positioning assembly. To check the reliability of this method certain measurements were compared between the patients' faces and the constructed 3D models.

Results: Excellent agreement was found in all measurements except for the "Inter-pupillary width" and the "Frontal prominence".

Conclusions: The presented technique proved to be an accurate, reproducible and economic method for 3D model construction.

Keywords: Facial esthetics; Facial Perception; 3D imaging; Diagnosis.

*Corresponding Author:

Heba M. Dehis BDs, Msc,

Assistant Lecturer, Faculty of Oral and Dental Medicine, Department of Orthodontics and Dentofacial Orthopedics, Cairo University, Egypt.

Tel: (02) 01020490611

E-mail: hebadehis@hotmail.com and heba.dehis@dentistry.cu.edu.eg

Received: May 12, 2015

Accepted: June 19, 2015

Published: June 23, 2015

Citation: Dehis HM, El-Sharaby FA, Mostafa YA (2015) 3D Soft Tissue Imaging: An Accurate and Economical Approach. *Int J Dentistry Oral Sci.* 2(6), 87-93. doi: <http://dx.doi.org/10.19070/2377-8075-1500019>

Copyright: Heba M. Dehis[©] 2015. This is an open-access article distributed under the terms of the Creative Commons Attribution License, which permits unrestricted use, distribution and reproduction in any medium, provided the original author and source are credited.

Introduction

Soft tissue appearance represents the primary concern among individuals seeking orthodontic treatment. Studies have shown that soft tissue profile and facial esthetics should be the primary concern when planning for treatment. Assessment of facial appearance, although clearly a 3-dimensional (3D) problem, has been attempted with two dimensional (2D) methods [1]. Moreover,

limited research work was found dealing with facial assessment based on 3D imaging techniques, due to the invasiveness and the high expenses of most of the 3D imaging modalities.

Computed Tomography (CT) and Magnetic resonance 3D imaging (MRI) provide a relatively accurate 3D method. Unfortunately, both techniques are expensive and impractical for everyday use, together with the fact that CT is highly invasive.

Other recent techniques include, morphanalysis [2], laser scanning [3, 4], stereolithography [5], 3D ultrasonography [6], 3D facial morphometry [7, 8], digigraph imaging [9], Moiré topography [10], contour photography [11] and "Stereophotogrammetry" [12]. These techniques are non-invasive, but some of them lack accuracy, while others are highly expensive, time consuming and non-practical [13].

Accordingly, there is a need for a simpler, accurate, less costly and practical technique whereby, we would be able to assess the soft tissue and facial features, thus raising the standard of care delivered to our patients. The aim of the current study was to develop a new, accurate and economic method for 3 dimensional (3D) soft tissue image construction, hence researchers can utilize this technique and be able to analyze soft tissue facial features three dimensionally.

Materials and Methods

The sample of this study comprised ten adult females. For each subject, a 3D video model was constructed based on facial measurements taken after patient positioning using custom made patient positioning assembly.

Patient positioning assembly

A chair specially designed for this study was constructed. The chair included the following parts (Figures 1,2):

The seat part: Consisted of a rounded pad that rotates freely around a vertical axis. Five wings with vertical slots were soldered to the vertical axis, so that a 45 degrees angle was maintained between each wing. The patient position was confirmed by locking the seat part using a specially fabricated locking lever inserted in each wing slot.

Back support: Consisted of two parts.

Small rigid bar; with one end soldered at a right angle to the vertical axis, and the other end consisted of a hollow tube with a tightening screw.

Long rigid bar; which extended vertically perpendicular to the floor and parallel to the vertical axis, with one end inserted in the tube of the small rigid bar moving freely so that it can be customized for each patient by sliding it through the tube and locking with the tightening screw. The head support was attached to the other end of the long rigid bar.

Head support: To assure the proper support of the patient's head, a wooden U- shaped head rest was fabricated, which in turn was attached to the long rigid bar of the back support.

Cephalostat: Cephalostat used for capturing the lateral cephalometric radiographs was used to ensure a proper and standardized head support. The cephalostat was modified in order to allow for patient rotation with the patient positioning assembly (Figure 3).

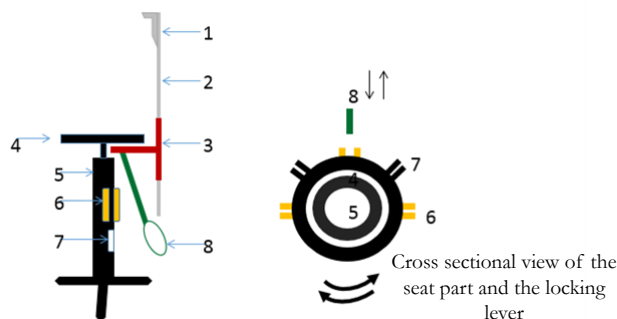
Certain landmarks on the patients' faces were used to act as guidelines for checking the reproducibility and accuracy of the constructed 3D video model [14] (Table 1).

A high quality digital camera * was used to capture the photographs. To assure high precision and accuracy, the camera was adjusted in three planes.

Figure 1. Patient positioning assembly.



Figure 2. A diagram representing the different components of the "Patient positioning assembly".



1. Head support.
2. Back support (Long rigid bar).
3. Back support (Short rigid bar).
4. Seat part (Rounded pad)
5. Seat part (Vertical axis).
6. 90 degrees wing slot.
7. 45 degrees wing slot.
8. Locking lever.

Figure 3. Cephalostat used to support the patient’s head in the natural head position.

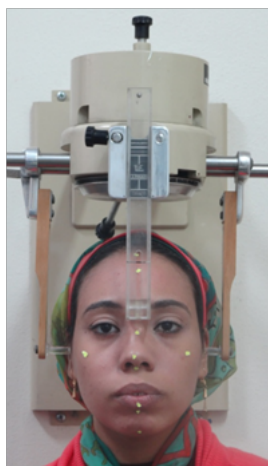


Table 1. Frontal faciometric landmarks.

Midline Landmarks (arranged from top to bottom)	
Trichion(Tc)	The most anterior midline point on the hairline
Soft tissue glabella (Gl)	The most prominent midline point on the forehead
Soft tissue nasion (N)	The most concave midline point in the frontal aspect of the bridge of the nose
Pronasale (Pn)	The most prominent midline point on the tip of the nose
Subnasale (Sn)	The midpoint of the angle at the columella base where the lower border of the nasal septum and surface of the upper lip meet; not identical to the bony point ANS or nasospinale. ^(Turkai)
Upper stomion (USt)	The most inferior midline point on the upper lip.
Lower stomion (LSt)	The most superior midline point on the lower lip.
Vermillion inferius (VI)	The most inferior midline point on the vermilion border of the lower lip.
Soft tissue B (b)	The deepest midline point on the concavity between the lower lip and chin.
Soft tissue menton (Mt)	The most inferior midline point on the chin.
Bilateral Landmarks (arranged from top to bottom)	
Endocanthion (En)	The medial canthus of the eye
Exocanthion (Ex)	The lateral canthus of the eye
Pupil (P)	The center of the pupil
Cheek prominence (Cp)	The most prominent point on the cheek
Tragion (Tg)	The center of the tragus of the ear
Chelion (Ch)	The corner of the lips

Vertical: Adjustments were made so that the center of the camera lens maintained a vertical distance from the floor, equal to that measured from the tip of the nose of each patient to the floor.

Antero-posterior: A constant distance (2 feet) was maintained from the camera to the center of the chair.

Horizontal: The camera was adjusted to be parallel to the plane being photographed (coronal, sagittal). This was achieved by the aid of a line being drawn on the floor, which was parallel to the mid plane of the patient.

After adjusting the patient positioning assembly, the cephalostat’s ear rods, and frontal rod were disengaged just before capturing the photographs. This was essential to be able to take all the face details to construct the 3D video model accurately.

For 3D image reconstruction five extra-oral photographs were

captured for each subject (Figure 4).

- a. Frontal at rest.
- b. 45 degrees at rest (Right side).
- c. Profile at rest (Right side): the patient was adjusted to be at exactly 90 degrees from the original frontal view, as confirmed by the chair.
- d. 45 degrees at rest (Left side).
- e. Profile at rest (Left side): 90 degrees from the original frontal view as confirmed by the chair.

Special software ** was employed for the current study in order to construct the 3D models for the patients. The following clinical measurements were needed during the construction procedure:

1. **Total facial height:** The linear measurement from the “Trichion”(I); hair line; to “Soft tissue Menton”(M); lowest point on the contour of the soft tissue chin [15].

2. **Zygomatic width:** The linear measurement between the right to the left soft tissue “zygion” (Zy); the most laterally suited point on the zygomatic arch [16].

Other measurements were taken to perform a frontal and lateral facial analysis, facial measurements taken directly on the patients were compared to those on the 3D models.

Frontal facial Feature Analysis (FFFA): This comprised the following measurements;

1. Interpupillar width (PR-PL)
2. Mouth width (ChR-ChL)
3. Intercanthus width (EnR-EnL)
4. Width of the eye (EnR-ExR)
5. Width of the eye (EnL-ExL)
6. ExR-TgR
7. ExL-TgL

Lateral Facial Feature Analysis (LFFA): This analysis included the following measurements;

1. Frontal prominence (Gl-Tg)
2. Prominence of the bridge of the nose (N-Tg)
3. Prominence of the tip of nose (Pn-Tg)
4. Cheek Prominence (Cp-Tg)
5. Forehead length (Tc-N)
6. Middle anterior facial height (N - Sn)
7. Lower anterior facial height (Sn - Mt)
8. Upper half of the lower face (Sn-VI)
9. Lower half of the lower face (VI-Mt)
10. Upper third of lower face (Sn- USt)
11. Lower lip height (LSt-mt)
12. Lower third of lower face (b-Mt)

An “Outside caliper” was used for these measurements (Figure 5).

3D model construction

The extra oral photographs were digitized, and trimmed a little behind the tragus of the ear and on the hairline. The photographs were used to construct the 3D models with the aid of the computer software** (Figure 6).

Statistical analysis

The data were collected, tabulated and analyzed. A reproducibility index, called the concordance index coefficient (CCC), introduced by Lin, was used. It evaluates the agreement between 2 readings (actual and 3D model) by measuring the variation for the 45° line through the origin (the concordance line). The CCC measurements are accurate and precise. In addition, Kappa Cohen test was performed to obtain inter-observer agreement by both actual and 3D model readings for each measurement.

Results

The results and comparisons between the actual facial measurements and digital models from frontal facial features analysis are shown in Table (2) and Figure (7). The results were compared for conformity and equivalency by using concordance correlation coefficient (CCC) and Pearson correlation coefficient (PCC) respectively.

Excellent agreement was obtained between both modalities for all elements except “Inter-pupillary” width as its error percentage between both readings was (14.77%) as listed in Table (2). Total error percentage between both readings were (5.07%) indicating that there was approximately Good agreement between both readings by using Kappa Cahen test for interobserver agreement, as listed also in Table (1).

On the other hand, the results and comparisons between the actual facial measurements and digital models from lateral facial features analysis are shown in Table (3) and Figure (8). Also, the results were compared for conformity and equivalency by using concordance correlation coefficient (CCC) and Pearson correlation coefficient (PCC) respectively.

Excellent agreement was obtained between both measuring modalities for all measuring elements except “Frontal prominence” as its error percentage was (-1.47) as listed in Table (3). Total error percentage between both readings were (1.81 %) indicating that there was approximately good agreement between both readings by using Kappa Cahen test for interobserver agreement, as listed also in Table (3).

Figure 4. Photographs taken before 3D image reconstruction.



(a): Frontal at rest, (b): 45 degrees (Right), (c): Profile (Right), (d): 45 degrees (Left), (e): Profile (Left)

Figure 5. Outside Caliper.



Figure 6. Screen shot of the 3D video model.

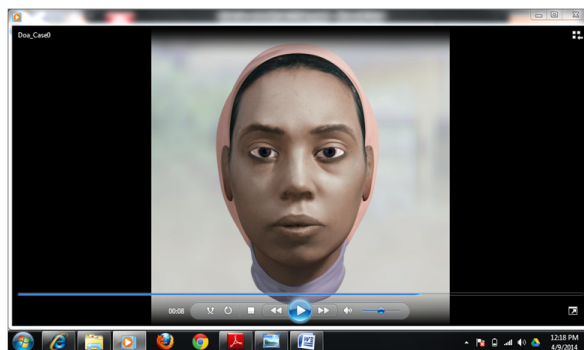


Figure 7. Scatter graph of method errors analysis of frontal facial features.

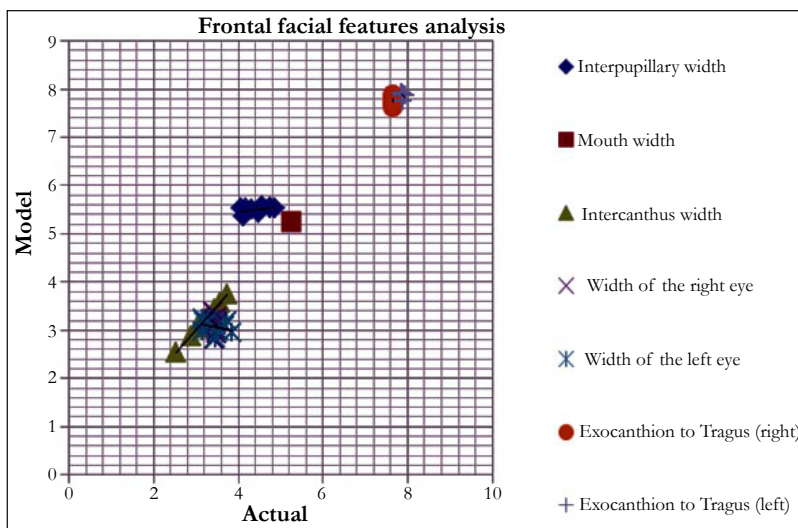


Figure 8. Scatter graph of method errors analysis of lateral facial features.

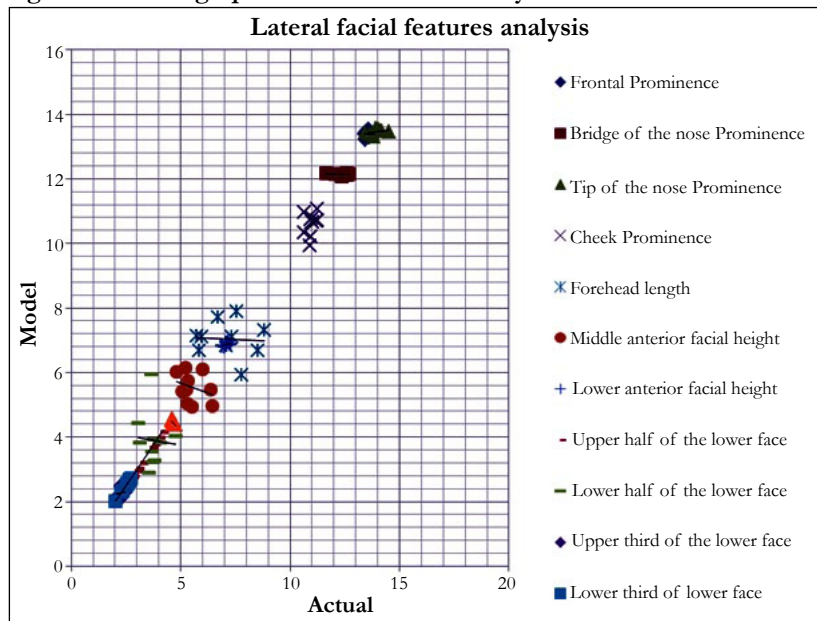


Table 2. Analysis of method errors of frontal facial features.

Frontal Facial Feature Analysis (FFFA):	Actual	Model	CCC	PCC	Error %	Total error %	κ	Inter-observer Agreement
	Mean ± SD	Mean ± SD						
1- Interpupillary width	4.4 ± 0.42	5.05 ± 0.071	0.556*	0.498	14.77	5.07	-5.7	No Agreement
2- Mouth width	5.25 ± 0.002	5.254 ± 0.002	0.778**	0.108	0.08		0.26	Good Agreement
3- inter-canthus width	3.347 ± 0.424	3.347 ± 0.42	1.524**	1	.00		0	Agreement by chance
4- Width of the eye (right)	3.45 ± 0.071	3.1 ± 0.14	0.847**	-0.272	-10.14		.75	Good Agreement
5- width of the eye (left)	3.35 ± 0.212	3.1 ± 0.14	1.024**	-0.337	-7.46		.85	Good Agreement
6- Exocanthion to Tragus (right)	7.649 ± 0.0041	7.75 ± 0.071	0.877**	-0.298	1.32		.85	Good Agreement
7- Exocanthion to Tragus (left)	7.885 ± 0.021	7.75 ± 0.071	1.012	-0.43	-1.71		.62	Good Agreement

CCC; Concordance index Coefficient, PCC; Pearson's Correlation Coefficient, K; Kappa Cohen factor

*P<0.75; fair agreement

**P>0.75; excellent agreement

Table 3. Analysis of method errors of lateral facial features.

Lateral Facial Feature Analysis (LFFFA):	Actual	Model	CCC	PCC	Error %	Total error %	κ	Inter-observer Agreement
	Mean ± SD	Mean ± SD						
1- Frontal Prominence (Glabella to Tg)	13.6 ± 0.14	13.4 ± 0.14	0.211*	-0.003	-1.47	1.81	-1.2	No Agreement
2- Prominence of the bridge of the nose (N to Tg)	12.35 ± 0.28	12.125 ± 0.035	0.879**	-0.248	-1.82		.90	Good Agreement
3- Prominence of the tip of the nose (PN to Tg)	13.75 ± 0.35	13.45 ± 0.07	0.814**	0.444	-2.18		.15	Good Agreement
4- Cheek Prominence (Cheek prominence to Tg)	11 ± 0.25	10.675 ± 0.46	1.056**	0.283	-2.95		.35	Good Agreement
5- Forehead Length (Trichion to Nasion)	7.15 ± 0.92	7.125 ± 0.95	0.922**	-0.069	-.35		.10	Good Agreement
6- Middle anterior facial height (N to S.N)	5.75 ± 0.78	5.55 ± 0.49	0.914**	-0.3	-3.48		.35	Good Agreement
7- Lower anterior facial height (S.N to M')	7 ± 0.14	6.85 ± 0.06	0.974**	0.448	-2.14		.70	Good Agreement
8- Upper half of the lower face (S.N to V. border)	3.45 ± 0.49	3.45 ± 0.49	1.74**	1	.00		0	Agreement by chance
9- Lower half of the lower face (V. inferior to M')	3.6 ± 0.42	3.7 ± 0.57	0.846**	-0.067	2.78		.80	Good Agreement
10- Upper third of the lower face (S.N to U. Stom)	2.3 ± 0.14	2.305 ± 0.13	0.932**	0.117	.22		0.31	Good Agreement
11- Lower lip height (L. Stomion to M')	4.65 ± 0.045	4.45 ± 0.071	0.945**	-0.532	-4.30		.25	Good Agreement
12- Lower third of lower face (B' to M')	2.4 ± 0.28	2.4 ± 0.28	0.822**	1	.00		0	Agreement by chance

CCC; Concordance Index Coefficient, PCC; Pearson's Correlation Coefficient, K; Kappa Cohen factor

*P<0.75; fair agreement

**P>0.75; excellent agreement

Discussion

3D imaging and assessment of facial esthetics has been approached by different studies [1-12]. This study was designed aiming to overcome the problems encountered in previous 3D imaging techniques, and to produce a new, accurate and economical method for 3D soft tissue image construction.

A “patient positioning assembly” specially designed for this study has been constructed to assure standardization of patient positioning during photographing, together with maintaining the same position at different views. Moreover, further standardization was assured by taking the patients’ photographs in the “Natural Head Position” as reported by previous studies [17-21]. This was guaranteed by the aid of the cephalostat in the patient positioning assembly.

Photographs at five different views were taken for each patient; frontal at rest, profile at rest (right), 45 degrees at rest (right), profile at rest (left) and 45 degrees at rest (left); to construct full facial image. Previous studies, which focused on facial analysis and manipulation of facial features to evaluate perception, depended only on 2D images whether profile photographs [17-24], three-quarter-view, smiling and non-smiling facial photographs [25], while Seager et al., (2008) [26] used 3d MD camera capture system to capture full facial images from ear to ear and under the chin.

The results of the current study showed excellent agreement between the actual facial measurements and the constructed 3D model in all measurements of the (FFFA) except for the “Inter-pupillary width”. This could be due to the difficulty in taking this measurement without the patient moving his eyes.

Despite the fact that all measurements had excellent agreement yet two of them were highly accurate than others and had greater reproducibility, these were the “Mouth width” and the “Inter-canthus width”. Accordingly, the technique used in the current study was reliable especially at the oral and circum-oral region.

As regards the (LFFA), results showed as well that excellent agreement was achieved for all measurements except for the “Frontal prominence”, which was surprising and unexpected, as the points were marked on the patients’ faces. But this could be explained by the fact that the tragus is a soft movable tissue and could have been moved by pressure from the outside caliber used during measurements.

Inter-observer difference was tested, and showed that good agreement was found for all (FFFA), and (LFFA) of all patients, except for the “Inter-pupillary” and “Frontal prominence” measurements. This was predictable because measurements were taken by both observers without marking the points in advance, together with the difficulty in registering the “Inter-pupillary” width due to frequent eye mobility.

Conclusion

Based on the results of the current study, the presented technique proved to be an accurate, reproducible and economic method for 3D model construction.

References

- [1]. Ayoub AF, Wray D, Moos KF, Siebert P, Jin J, et al. (1996) Three-dimensional modeling for modern diagnosis and planning in maxillofacial surgery. *Int J Adult Orthod Orthognath Surg* 11(3): 225–233.
- [2]. Rabey G (1971) Craniofacial morphanalysis. *Proc R Soc Med* 64(2): 103–111.
- [3]. McCance AM, Moss JP, Wright WR, Linney AD, James DR (1992) A three-dimensional soft tissue analysis of 16 skeletal Class III patients following bimaxillary surgery. *Br J Oral Maxillofac Surg* 30(4): 221–232.
- [4]. Moss JP, McCance AM, Fright WR, Linney AD, James DR (1994) A three-dimensional soft tissue analysis of fifteen patients with Class II, Division 1 malocclusions after bimaxillary surgery. *Am J Orthod Dentofacial Orthop* 105(5): 430–437.
- [5]. Bill JS, Reuther JF, Dittmann W, Kübler N, Meier JL, et al. (1995) Stereolithography in oral and maxillofacial operation planning. *Int J Oral Maxillofac Surg* 24(1 Pt 2): 98–103.
- [6]. Hell B (1995) 3D sonography. *Int J Oral Maxillofac Surg* 24(1 Pt 2): 84–89.
- [7]. Ferrario VF, Sforza C, Serrao G, Puleto S, Bignotto M, et al (1994) Comparison of soft tissue facial morphometry in children with Class I and Class II occlusions. *Int J Adult Orthod Orthognath Surg* 9(3): 187–194.
- [8]. Ferrario VF, Sforza C, Poggio CE, Serrao G, Miani A Jr (1994) A three-dimensional study of sexual dimorphism in the human face. *Int J Adult Orthod Orthognath Surg* 9(4): 303–310.
- [9]. Nanda RS, Ghosh J, Bazakidou E (1996) Three-dimensional facial analysis using a video imaging system. *Angle Orthod* 66(3): 181–188.
- [10]. Kawai T, Natsume N, Shibata H, Yamamoto T (1990) Three-dimensional analysis of facial morphology using moire stripes. Part I. Method. *Int J Oral Maxillofac Surg* 19(6): 356–358.
- [11]. Leivesley WD (1983) The reliability of contour photography for facial measurements. *Br J Orthod* 10(1): 34–37.
- [12]. Burke PH, Beard FH (1967) Stereophotogrammetry of the face. A preliminary investigation into the accuracy of a simplified system evolved for contour mapping by photography. *Am J Orthod* 53(10): 769–782.
- [13]. Hajeer MY, Ayoub AF, Millett DT, Bock M, Siebert JP (2002) Three-dimensional imaging in orthognathic surgery: the clinical application of a new method. *Int J Adult Orthod Orthognath Surg* 17(4): 318–330.
- [14]. El-Mangoury NH, Mostafa YA, Rasmey EM, Salah A (1996) Faciometrics: A new syntax for facial feature analysis. *Int J Orthod Orthognath Surg* 11(1): 71–82.
- [15]. Jacobson A, Jacobson RL (2006) Radiographic Cephalometry: From Basics to 3-D Imaging. (2nd Ed), Quintessence Publishing, Chicago 19: 206.
- [16]. Jacobson A, Jacobson RL (2006) Radiographic Cephalometry: From Basics to 3-D Imaging. (2nd Ed), Quintessence Publishing, Chicago 22: 253.
- [17]. Giddon DB, Bernier DL, Evans CA, Kinchen JA (1996) Comparison of two computer animated imaging programs for quantifying facial profile preference. *Percept Mot Skills* 82(3 Pt 2): 1251–1264.
- [18]. Giddon DB, Sconzo R, Kinchen JA, Evans CA (1996) Quantitative comparison of computerized discrete and animated profile preferences. *Angle Orthod* 66(6): 441–448.
- [19]. Arpino VJ, Giddon DB, BeGole EA, Evans CA (1998) Presurgical profile preferences of patients and clinicians. *Am J Orthod Dentofacial Orthop* 114(6): 631–637.
- [20]. Hier LA, Evans CA, Begole EA, Giddon DB (1999) Comparison of preferences in lip position using computer animated imaging. *Angle Orthod* 69(3): 231–238.
- [21]. Kazandjian S, Sameshima GT, Champlin T, Sinclair PM (1999) Accuracy of video imaging for predicting the soft tissue profile after mandibular set-back surgery. *Am J Orthod Dentofacial Orthop* 115(4): 382–389.
- [22]. Soh J, Chew MT, Wong HB (2005) A comparative assessment of the perception of chinese facial profile esthetics. *Am J Orthod Dentofacial Orthop* 127(6): 692–699.
- [23]. Soh J, Chew MT, Wong HB (2005) Professional assessment of facial profile attractiveness. *Am J Orthop Dentofacial Orthop* 128(2): 201–205.
- [24]. Chan EK, Soh J, Petocz P, Darendeliler MA (2008) Esthetic evaluation of Asian-Chinese profiles from a white perspective. *Am J Orthod Dentofacial Orthop* 133(4): 532–538.
- [25]. Tatarunaite E, Playle R, Hood K, Shaw W, Richmond S (2005) Facial attractiveness: A longitudinal study. *Am J Orthod Dentofacial Orthop* 127(6): 676–682.
- [26]. Seager DC, Kau CH, English JD, Tawfik W, Bussa HI, et al (2009) Facial morphologies of an adult Egyptian population and an adult Houstonian white population compared using 3D imaging. *Angle Orthod* 79(5): 991–999.